Radio Science, Volume 23, Number 1, Pages 59–73, January–February 1988

A systematic error in MST/ST radar wind measurement induced by a finite range volume effect 1. Observational results

Shoichiro Fukao, Toru Sato, Peter T. May, Toshitaka Tsuda, and Susumu Kato

Radio Atmospheric Science Center, Kyoto University, Japan

Motoyuki Inaba and Iwane Kimura

Department of Electrical Engineering, Kyoto University, Japan

(Received September 17, 1986; revised July 15, 1987; accepted October 19, 1987.)

Wind measurement by MST/ST radars may be accompanied by a systematic error due to a finite range volume effect which works when a thin turbulent layer is simultaneously located in several adjacent range volumes. The error occurs when the layer coincides with a cross section through the range volume which is not symmetric with respect to the center of the beam. The finite range volume effect appears as a false vertical shear of horizontal wind in a vertical scale of the order of a few hundred meters, even if the ambient wind field is uniform. The false wind shear sometimes exceeds 40 ms^{-1} km^{-1} in magnitude or the critical value to induce the Kelvin-Helmholtz instability. Also the effect leads to a false temporal variation of the wind measurement, although the wind field does not change at all. The false wind shear with a magnitude less than 40 ms^{-1} km^{-1} cannot be discriminated from a true one in the observed data. It seems hard to indicate directly that the finite range volume effect appears as theoretically conceived. Judging from wind velocity and echo intensity data obtained by the MU radar in Japan, this effect appears quite frequently in the atmosphere. The small vertical scale wind shear as well as the temporal variation found only at a specific range should be treated with great care except when the ambient wind field is weak, where the finite range volume effect is not so important.

1. INTRODUCTION

Remote sensing of winds and turbulence in the middle atmosphere (height range of 10–100 km) by the Doppler technique is widely incorporated by MST/ST radars [e.g., *Balsley and Gage*, 1980; *Gage and Balsley*, 1984; *Röttger*, 1984]. Radial wind velocities measured in three or more beam directions are used to infer the three dimensional wind field, assuming that the wind field is uniform in the region where the antenna beam is steered. This technique provides wind profiles which are, in general, consistent with the meteorological wind measurements by rawinsondes and rocketsondes concurrently made near the radar sites [e.g., *Balsley and Gage*, 1980; *Fukao et al.*, 1982, 1985*b*; *Warnock et al.*, 1978]. However, the assumption of wind uniformity has not yet thoroughly been verified experimentally. Rather, there seems to exist short period fluctuations with spatial scales less than the distance between the beam positions [*Waterman et al.*, 1985]. These fluctuations certainly deteriorate the wind velocity estimation [*Fukao et al.*, 1988]. Further error would also be caused by the wind nonuniformity within the range volume which is principally determined by antenna aperture, transmitted pulse width, and sampling range gate [*Chang*, 1980].

In this paper we wish to show that a systematic error in the wind velocity estimation may occur due to a finite range volume effect. This error, which can occur even in uniform wind fields, leads to false wind shears and/or false temporal variations of wind which do not exist in the real wind field. The effect of this error seems to be very complicated, since it is sometimes difficult to discern the true wind shear from the false one in the observed wind data. This paper will focus on the observational features of this error, and its quantitative discussion will be given in the accompanying paper [*Fukao et al.*, this issue].

Some previous studies have also been performed concerning some effects of a non-uniform "filling" of the range volume by turbulence on wind measure-

Paper number 7S0827.
0048-6604/88/007S-0827$08.00

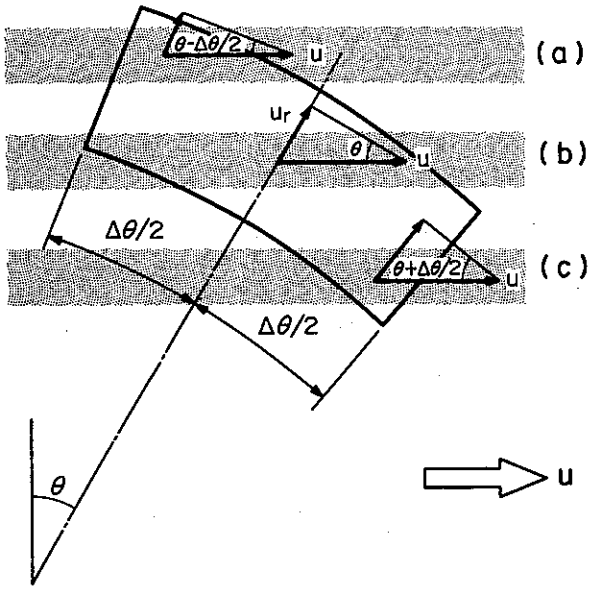

Fig. 1. Vertical cross section of a range volume illuminated by the antenna beam of MST/ST radars (encircled by thick line). The beam is assumed to be tilted in a plane parallel to the ambient horizontal wind u; θ is the zenith angle of the apex (chain line) of the antenna beam with one-way half-power width of $\Delta\theta$. A thin horizontal turbulent layer shown by shade is assumed to be located at either 1*a*, 1*b* or 1*c*.

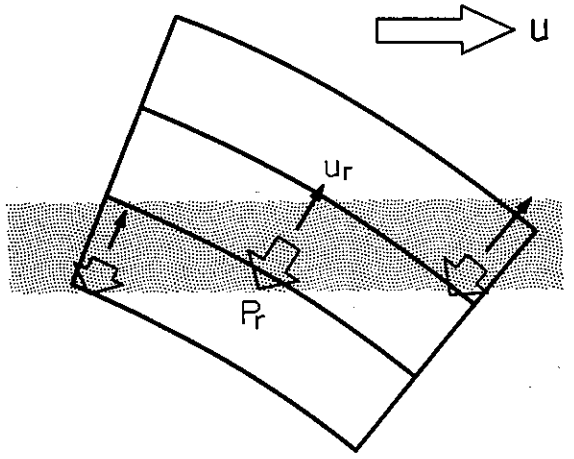

Fig. 2. A thin turbulent layer shown by shade is assumed to be located simultaneously in three adjacent range volumes. Thin arrows show the radial velocity or projection of the horizontal wind velocity observed at the respective range volumes, while thick arrows give echo intensity.

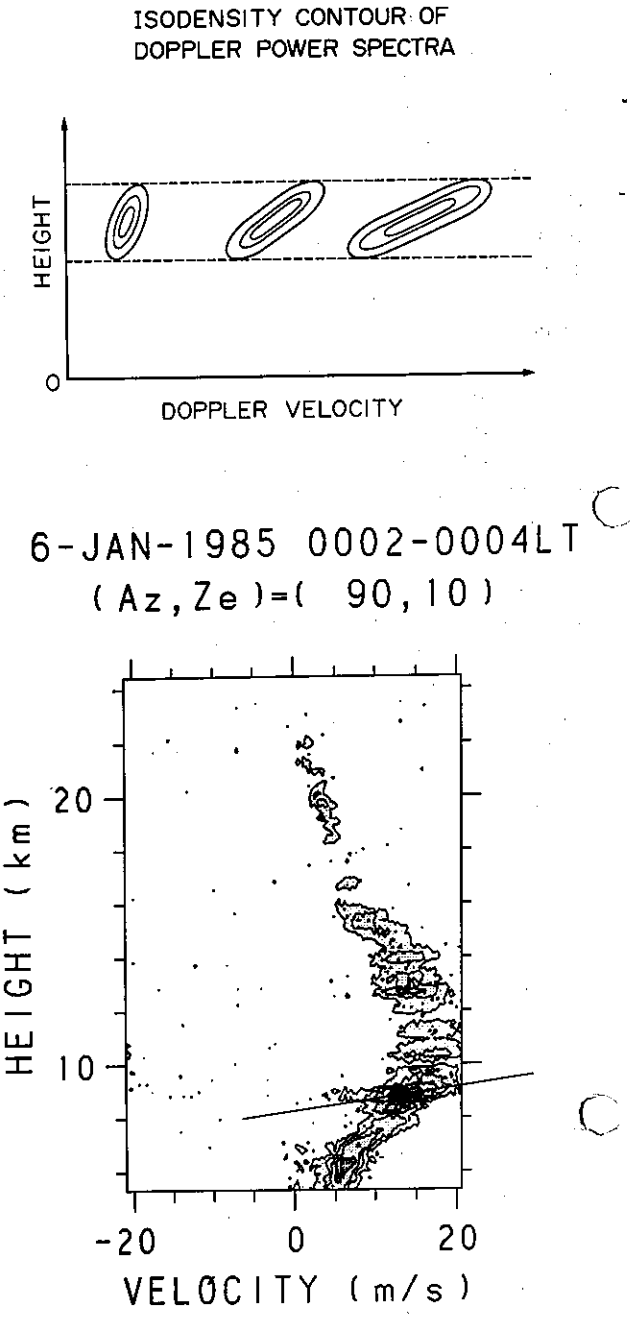

Fig. 3. (*a*) Schematic diagram of isodensity contour of Doppler power spectra, that is, the spectral density as a function of frequency and height for scatter from a single layer. Examples for three mean wind speeds are shown. (*b*) Isodensity contour of Doppler power spectra observed by the MU radar for an approximately 2-min period of 0002–0004 LT (LT is local time (Japan Standard Time)) on January 6, 1985. The antenna beam is directed 10° from the zenith toward the east (90° in azimuth from the north).

ments [*Atlas et al.*, 1969] and the observed spectral width [e.g., *Atlas et al.*, 1969; *Hocking*, 1983]. However, in the case of MST/ST radars these effects may be severe in many cases as will be shown.

All observational results were obtained with the aid of the MU radar located at Shigaraki, Japan (34.85°N, 136.10°E). This radar is a 46.5 MHz radar using an active phased array system [*Kato et al.*, 1984; *Fukao et al.*, 1980, 1985*a*, *b*]. The peak and average radiated powers of the whole system are 1.0 MW and 50 kW, respectively. The antenna aperture is 8,330 m^2, providing a main beam of 3.68° in one-way half-power width. This system makes it possible to steer the antenna beam up to 30° from the zenith in each interpulse period (IPP). In the observations related to the present work the transmitted pulse was a 16-element complementary code with 1-μs pulse width, corresponding to 150-m (range) resolution. The IPP was 400 μs. Unless otherwise mentioned, the data processing was made as follows: First, the echo was sampled at 128 heights spaced in a range of 5.4–24.5 km at 150-m intervals. Then, 128 point complex fast Fourier transforms were calculated in real time to obtain Doppler velocity spectra for each 9.7-s period. Finally, the resulting power spectra were averaged for approximately 2 min.

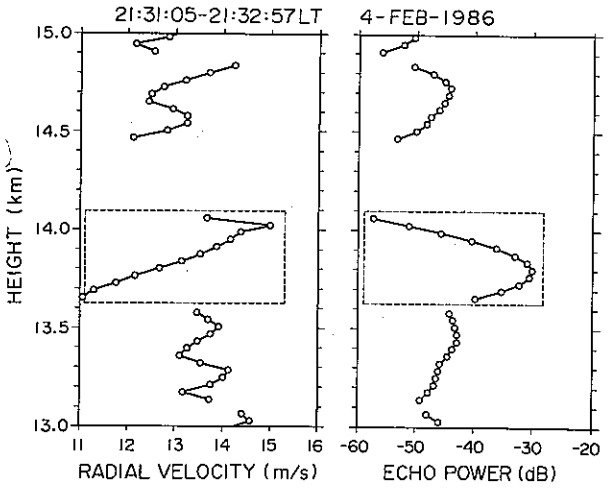

Fig. 4. Height profiles of radial wind velocity (left) and echo power (right) observed by the MU radar for an approximately 2-min period of 2131–2133 LT on February 4, 1986. The antenna beam was directed 10° from the zenith and 75° in azimuth from the north. A false wind shear seems to exist in a height range encircled by broken lines.

2. FINITE RANGE VOLUME EFFECT

Considerable evidence has so far been presented to indicate that stratospheric and some tropospheric turbulence occurs in vertically very thin (about 100 m or less) and horizontally extended layers, separated in height of a few hundred meters or more [e.g., *Woodman*, 1980]. In order that such layers be discriminated precisely, the range volume of the MST/ST radars has to be sufficiently small [e.g., *Chang*, 1980]. However, the turbulent layers are considered to be thinner than range resolutions in ordinary MST/ST radars.

The measured velocity is presumed to be an average of wind velocity within the range volume, where the radio wave scattering occurs. It should be noted that the average does not reflect the mean wind velocity in the range volume but is weighted by the turbulence intensity. Presumably, the inferred value represents the wind velocity at a specific height within the range volume where a turbulent layer is located [*Sato and Fukao*, 1982].

Referring to Figure 1, let u be the ambient horizontal wind which is uniform over a range volume encircled by thick line (no vertical wind is assumed), and the antenna beam be tilted by an angle of θ from the zenith toward the wind direction. Three cases in which a turbulent layer is located at different heights in a same range volume are considered. In case 1*b*, the scattering occurs at the center of the range volume, that leads to the observed radial velocity $u_r = u \sin \theta$. Thus the horizontal velocity is correctly estimated as $u = u_r/\sin \theta$ (As noted above the estimated horizontal velocity is really not the one determined at a specific point but an integrated one over the total range volume). On the other hand, the inferred horizontal velocities become $u \sin (\theta - \Delta\theta/2)/\sin \theta$ and $u \sin (\theta + \Delta\theta/2)/\sin \theta$ in case 1*a* and 1*c*, respectively, when the scattering occurs at the edges of half power width of the radar beam. The difference of the observed horizontal wind between 1*a* and 1*c* is estimated to be approximately 20 ms^{-1} for MST/ST radars with beam width ($\Delta\theta$) of 3°–4°, $\theta = 10°$, and $u = 50$ ms^{-1}, which is by no means negligibly small. Thus a wind estimation error is caused due to the finiteness of the range volume. In the following discussion, this effect is called finite range volume effect.

Range smearing due to range resolution was estimated by *Sato and Fukao* [1982], while range smearing due to antenna gain pattern was pointed out by *Watkins and Johnston* [1985]. However, the former did not discuss on the finite beam width, and the

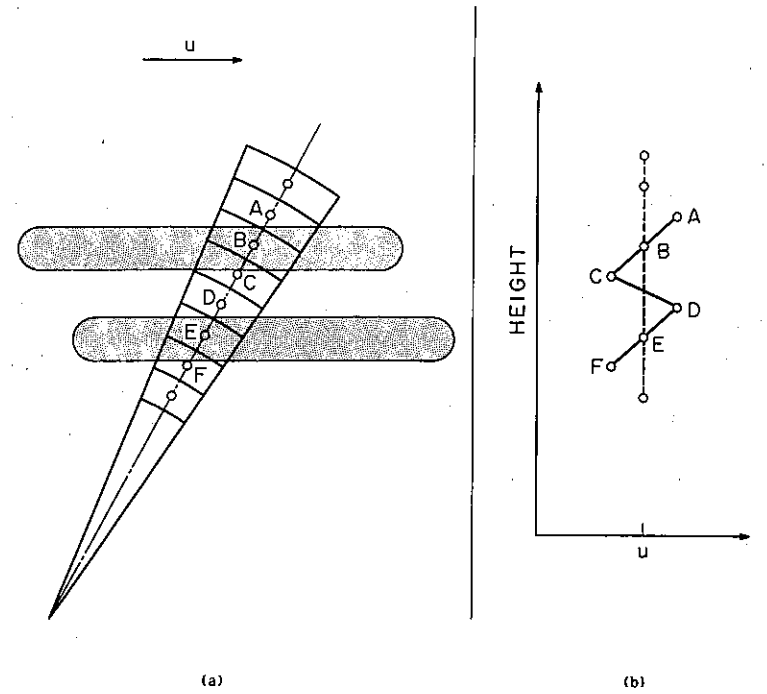

Fig. 5. Schematic diagram showing the finite range volume effect. (*a*) Vertical cross section of range volumes illuminated by antenna beam (encircled by thick line). Thin turbulent layers are indicated by shade. (*b*) Height profile of horizontal wind velocity to be observed in the case shown in 5*a*. Positive false shear appears in height ranges from *A* to *C* and from *D* to *F*, while a negative one in a height range from *C* to *D*.

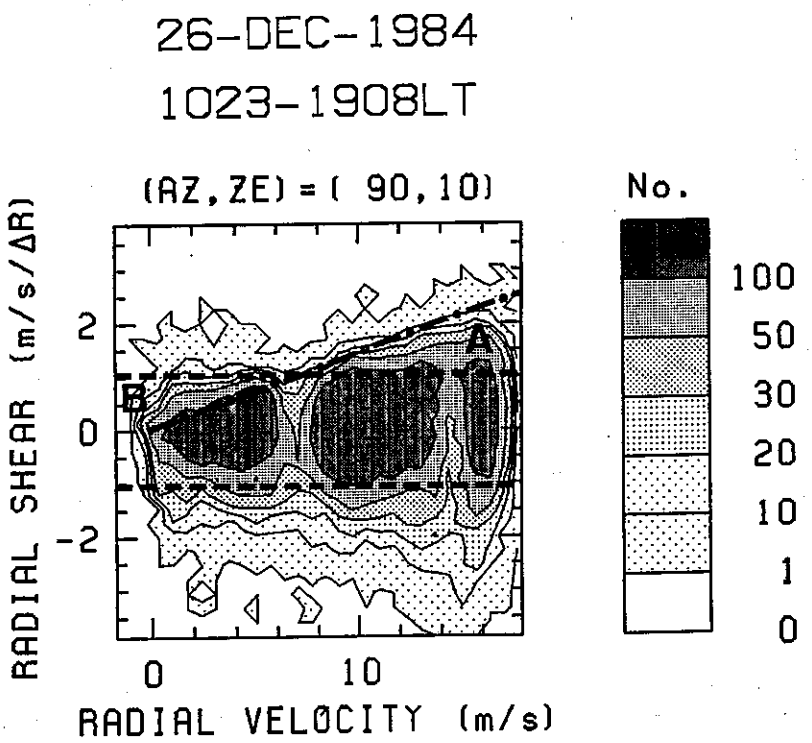

Fig. 6. Occurrence frequency distribution of radial-velocity shear versus radial velocity observed by the MU radar in a period 1023–1908 LT on December 26, 1984. The beam direction is the same as in Figure 3*b*. The contour levels for respective frequency are shown on the right hand side. Chain line is the maximum theoretical value, while broken lines are the critical values to generate the Kelvin-Helmholtz instability which correspond to a vertical shear in horizontal wind of approximately $\pm 40\ \mathrm{ms}^{-1}\ \mathrm{km}^{-1}$. See text for the regions of *A* and *B*.

latter did not extend their discussion to wind velocity estimation.

Now a turbulent layer with uniform intensity is assumed to be located, as an example, over three consecutive range volumes as shown in Figure 2. The magnitude of the radial velocity, and corresponding horizontal wind velocity, are observed to increase with increasing range notwithstanding the uniform ambient wind field. On the other hand, the echo intensity is observed to be a maximum at the center range volume where the major part of the turbulent layer exists. The observed echo intensity becomes less at the upper and lower range volumes. Consequently, isodensity contours of the observed Doppler power spectra are expected to be tilted as illustrated in Figure 3*a*, where the contour is given as functions of height (or range) and Doppler velocity (positive for leaving the radar). The tilt is enhanced for larger Doppler velocity as shown in the same figure. This is also true for the case that the wind direction and/or the beam direction is opposite. In a uniform wind field any beam directions except the vertical one are accompanied by this finite range volume effect. This feature is also true when the turbulent layer is simultaneously located over more than three range volumes.

Figure 3*b* is a 2-min averaged Doppler power spectrum obtained by the MU radar. It is demonstrated that many of the contours are tilted toward larger Doppler velocity, as theoretically expected in Figure 3*a*. The tilt near a height of 9 km is particularly prominent as indicated by the slope of thin solid line. It seems to appear more frequently above approximately 10 km where the wind velocity starts to decrease with height.

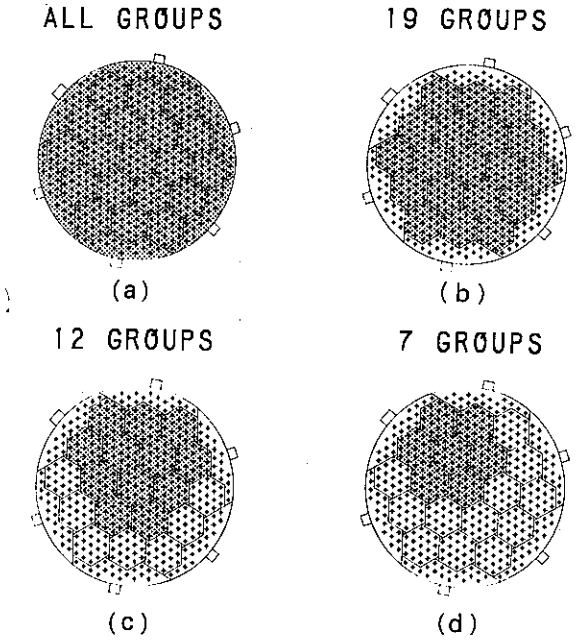

Fig. 7. Antenna array configuration of the MU radar. Plus ith square shows each antenna element, while six boxes outside ıe array accommodate the transmitter-receiver (TR) modules ɔnnected to individual antenna elements [*Fukao et al.*, 1985*a*]. he driven subarrays are indicated by shade. Number of driven ıbarrays are (*a*) 25 (all groups), (*b*) 19, (*c*) 12, and (*d*) 7, and the ɔrresponding beam widths are approximately 3.7°, 4.2°, 5.2° and 8°, respectively.

3. FALSE WIND SHEAR

The tilt of the Doppler spectral contour shown in Figure 3*b* indicates a small scale vertical shear of the horizontal wind. The wind shear presumably does not exist in the real wind field, but it is apparently induced by the finite range volume effect.

A typical false wind shear caused by the finite range volume effect is illustrated in Figure 4. The approximately 2-min height profiles of radial wind velocity and echo power data were obtained with the pulse scanning technique of *Röttger and Schmidt* [1979] using the MU radar. The echo was sampled with a stepwise delay of sampling by a quarter of the transmitted pulse or 0.25 μs, corresponding to a range step of 37.5 m. Since the delay was made every IPP, the normal 150-m range was scanned in four successive IPPs. The echo intensity height profile is given as a convolution of the shape of the transmitted pulse and intensity distribution of turbulence in the radial (beam) direction. If the turbulent layer is much thinner than the range resolution the shape of the echo power profile is similar to the shape of the transmitted pulse. On the other hand, in the case that the turbulent layer is extended in the range volume, the shape of the echo power profile is neither equal to the transmitted pulse nor to the turbulence intensity distribution [*Röttger and Schmidt*, 1979]. The echo intensity profile in a 450-m height range encircled by broken lines in Figure 4 resembles closely the transmitted pulse shape, suggesting that a very thin turbulent layer exists simultaneously in three adjacent range volumes. The inferred Doppler velocity has a larger shear as is consistent with the theoretical expectation, although the wind velocity change is fairly small both above and below this height range. This result is considered to be a manifestation of the finite range volume effect.

The maximum magnitude of the false radial shear of radial wind velocity (radial-velocity shear), Λ_r, that is expected in the geometry of Figure 2 is estimated as follows:

$$\Lambda_r = [u \sin(\theta + \Delta\theta/2) - u \sin(\theta - \Delta\theta/2)]/2/\Delta R$$
$$= u[\cos\theta \sin(\Delta\theta/2)/\Delta R] \quad (1)$$

where ΔR is range resolution. The scattering from both the top and bottom range volumes is assumed to occur principally at the edges of half power width of the antenna beam. Equation (1) indicates that Λ_r varies with θ, $\Delta\theta$, and ΔR in addition to u. Δ_r becomes 10 ms^{-1} km^{-1} for the same values of u, θ, $\Delta\theta$, and ΔR as used in section 2. This value corresponds to 60 ms^{-1} km^{-1} of vertical shear in the horizontal wind.

It should be added to note that the geometry

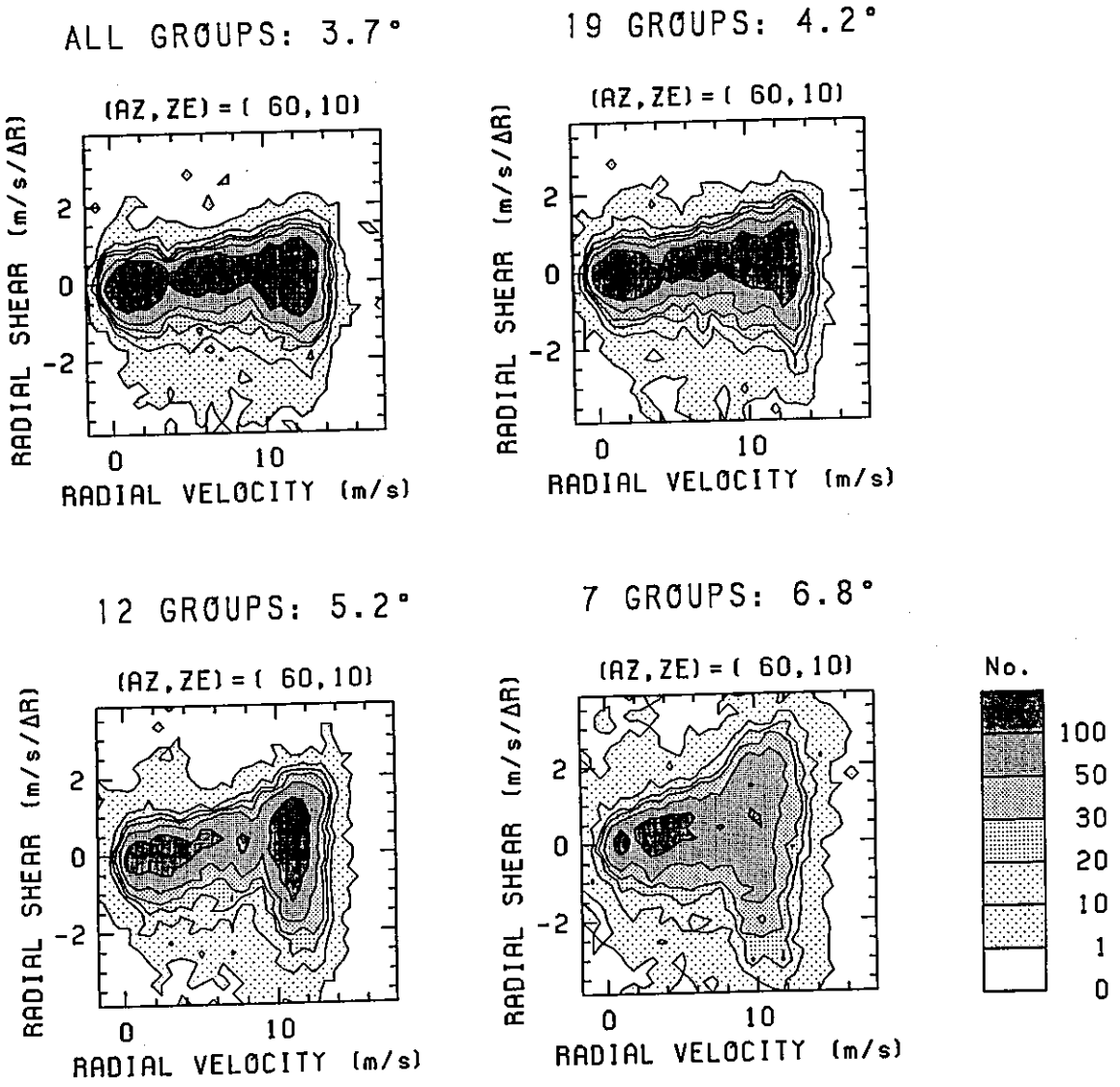

Fig. 8. Occurrence frequency distribution of radial-velocity shear versus radial velocity for the four different beam widths shown in Figure 7. The observation was made by the MU radar in a period from 1200 LT on December 15 to 0400 LT on December 16, 1985. The antenna beam was directed 10° from the zenith toward the east-northeast (60° in azimuth from the north). The contour levels for respective frequency are shown in the right bottom

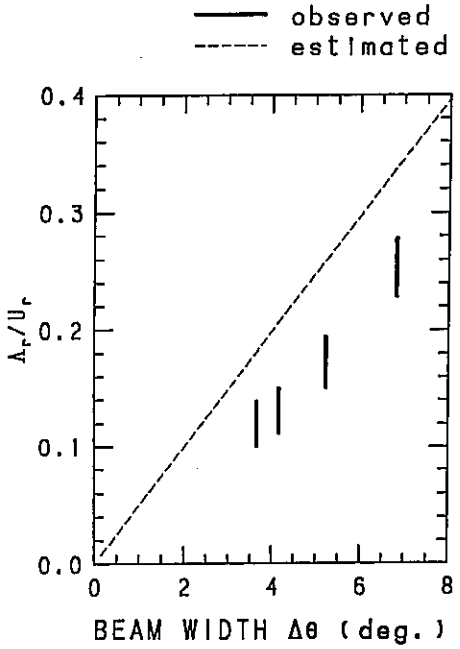

Fig. 9. The maximum shear-velocity ratio Λ_r/u_r versus beam width $\Delta\theta$. The vertical bars indicate the read error of the observed values shown in Figure 8, while the broken line is the theoretical maximum value.

shown in Figure 2 is an extreme case which uniquely defines the range R where the scattering occurs. For instance, R is defined as 24.1 and 16.3 km for $\theta = 10°$ and 15°, respectively. This geometry cannot be met except at these ranges, and above them Λ_r becomes smaller.

Considering the ordinary potential temperature gradient in the troposphere and stratosphere, wind shears with magnitude larger than approximately 40 ms^{-1} km^{-1} generate Kelvin-Helmholtz instability, which in turn reduces the magnitude of the original wind shear [e.g., *Klostermeyer*, 1980]. It is considered that wind shears of more than this critical value will generally be very rare in the real atmosphere. The theoretically expected maximum magnitude of 60 ms^{-1} km^{-1}, 1.5 times as large as the critical value, suggests that a large number of the observed wind shears occurring over small vertical scales over a few range volumes will be false.

False wind shear induced by a single turbulent layer always appears to be positive as schematically shown in a height range from A to C or from D to F in Figure 5. In the case that two thin turbulent layers

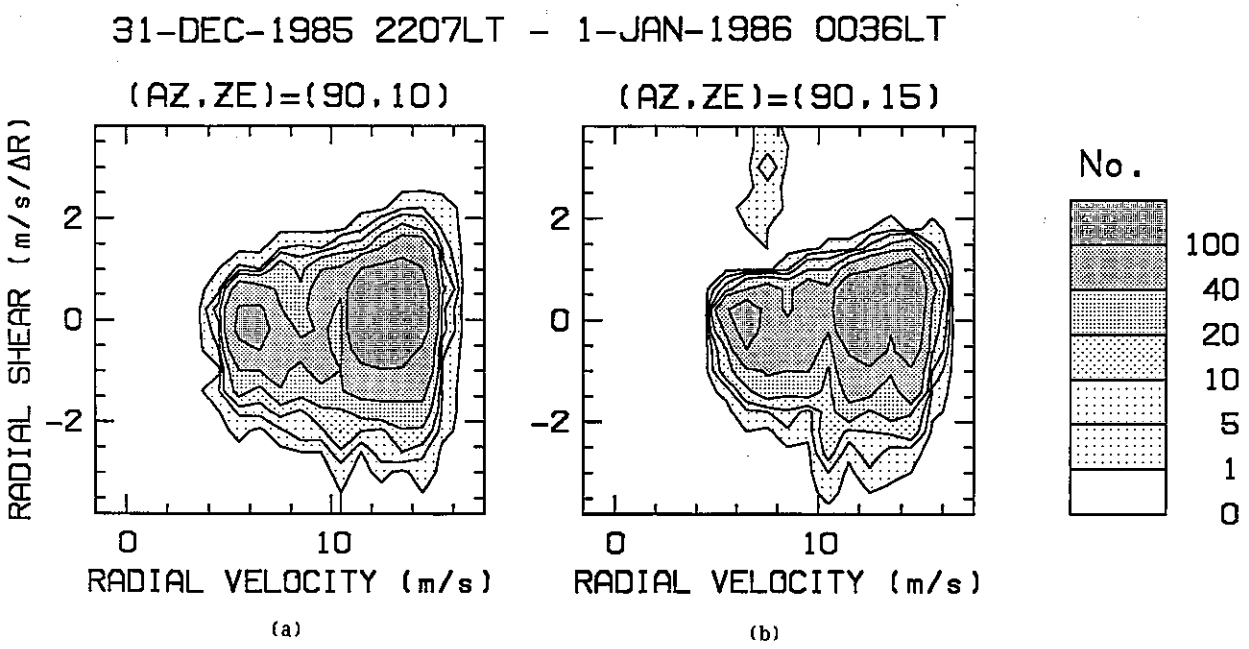

Fig. 10. Occurrence frequency distribution of radial-velocity shear versus radial velocity for two off-zenith angles of (*a*) 10° and (*b*) 15°. The contour levels for respective frequency are shown on the right-hand side. The observation was made by the MU radar from 2207 LT on December 31, 1985, to 0036 LT on Jaunuary 1, 1986. The antenna beam was directed toward the east (90° in azimuth from the north).

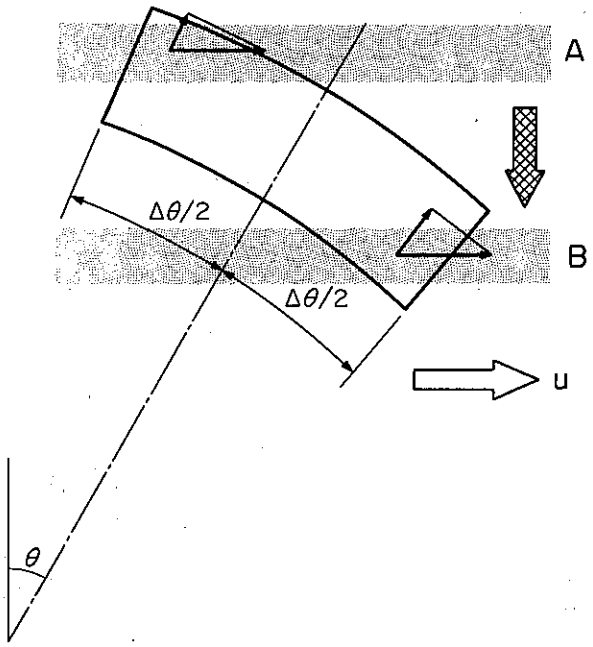

Fig. 11. Schematic diagram showing that a thin turbulent layer moves downward from height A to B with time within a same range volume.

exist simultaneously the wind velocity is apparently seen to decrease with height as shown in a height range from C to D. Also, the wind velocity will be interpreted to decrease with height if the correct wind values are estimated above or below the layers. This velocity decrease is falsely observed as a negative shear in a height profile of wind velocity. This false negative shear is not the one caused by the finite range volume effect, but is considered to accompany positive shears caused by the effect. Therefore the false negative shear will appear almost as frequently as the positive shear.

An occurrence frequency distribution of radial shear of radial wind velocity (radial-velocity shear) observed by the MU radar is shown in Figure 6. The occurrence frequency obtained in the upper troposphere and the lower stratosphere during an approximately 9-hour period is plotted in iso-frequency contours as functions of radial velocity (average of radial velocities at the upper and lower range volumes) and radial shear of radial velocity (difference of radial wind velocities at the two range volumes divided by $2\Delta R$). Magnitude of the shear is given in ms^{-1} per

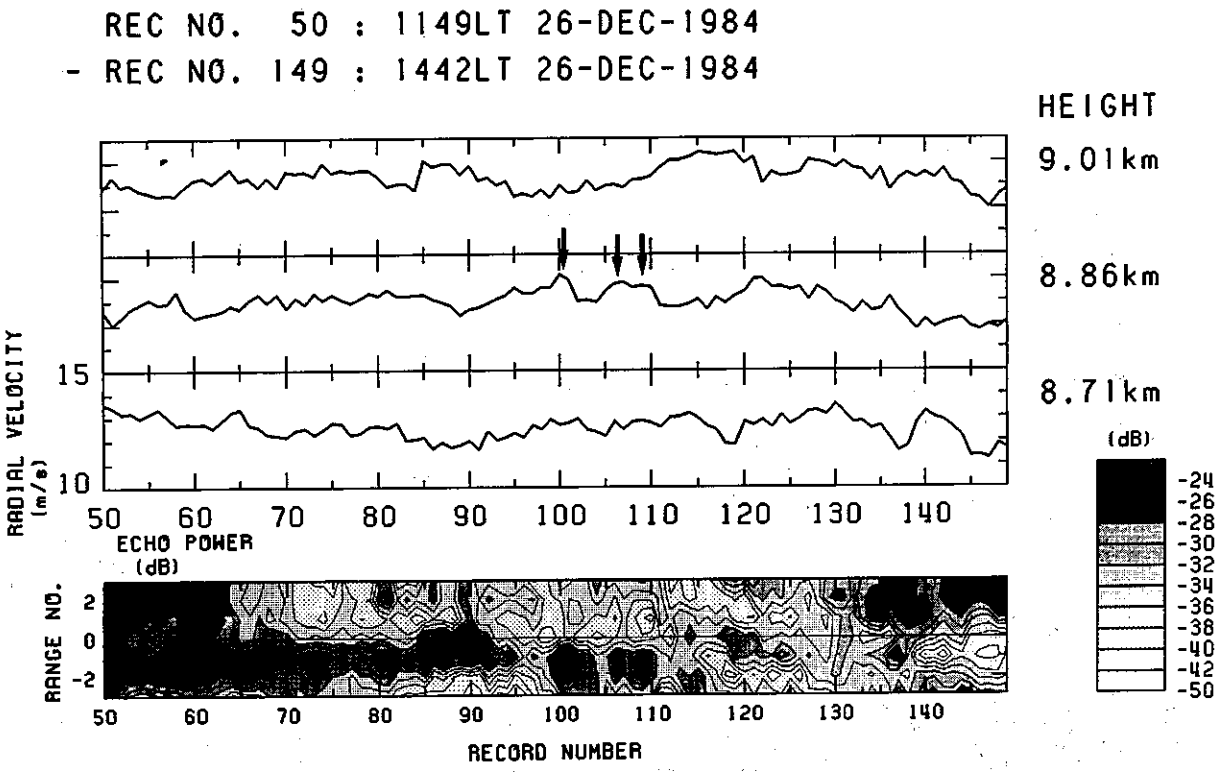

Fig. 12. (top) Temporal variation of radial wind velocity at three adjacent range volumes around 9.01, 8.86, and 8.71 km, respectively, during a period of 1149 to 1442 LT on December 26, 1984. The arrows indicate the instances when the finite range volume effect appears. (bottom) Temporal variation of echo power simultaneously observed at five adjacent range volumes including the three range volumes shown in the top diagram. The contour of echo intensity is given on the right-hand side.

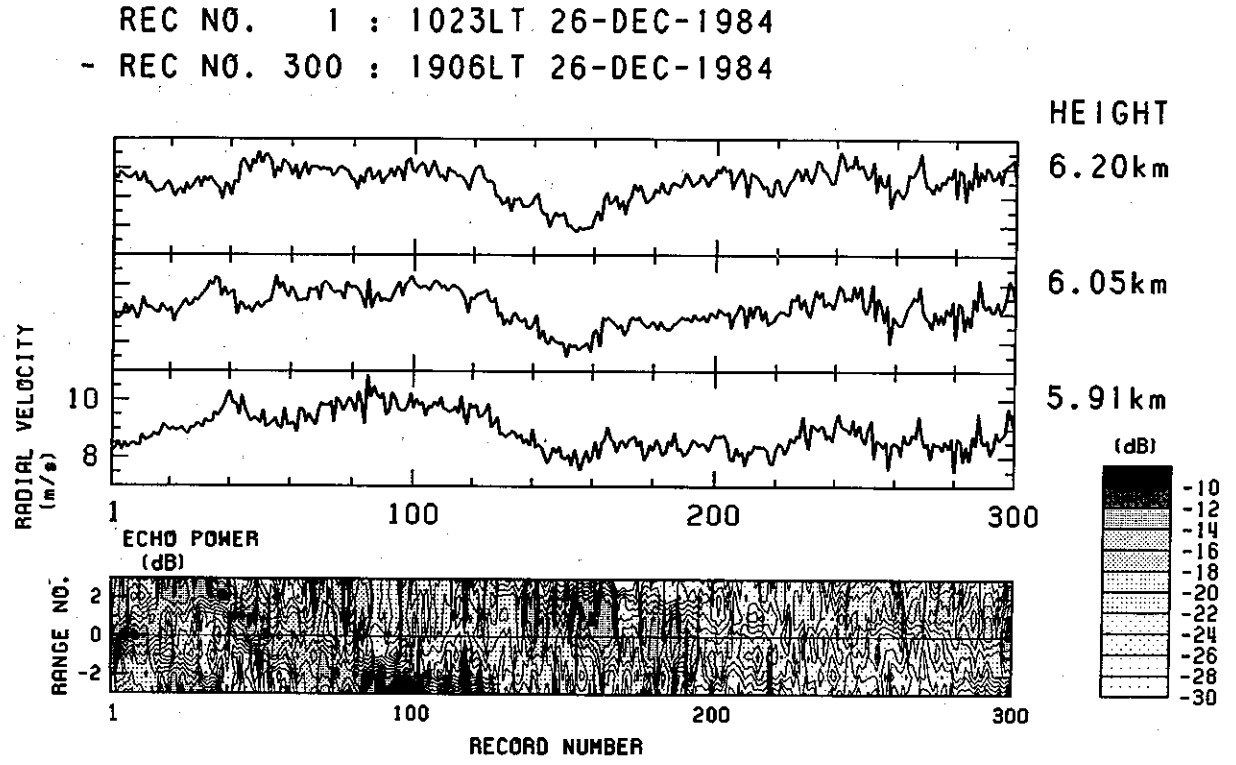

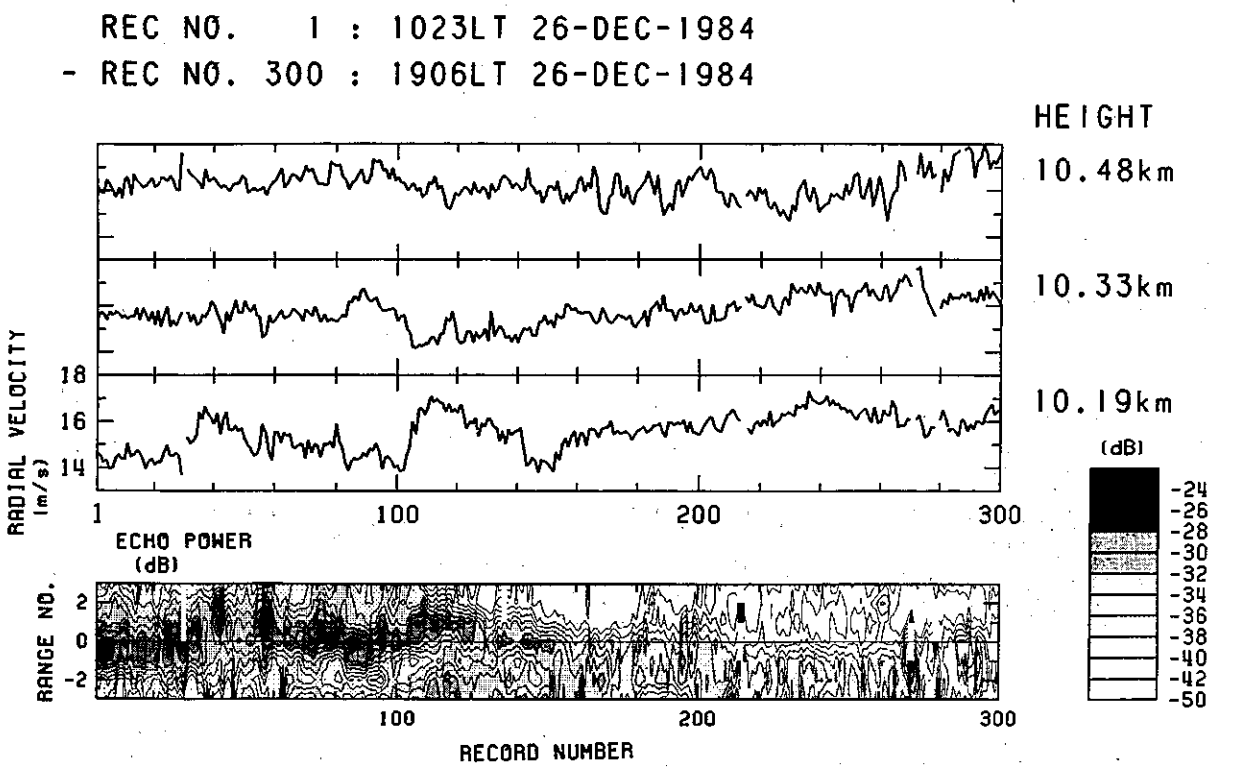

Fig. 13. (*a*) Same as Figure 12 except for height range and observational period. Note that the observational period is approximately three times larger than that of Figure 12. (*b*) Same as 13*a* except for height range and velocity scale.

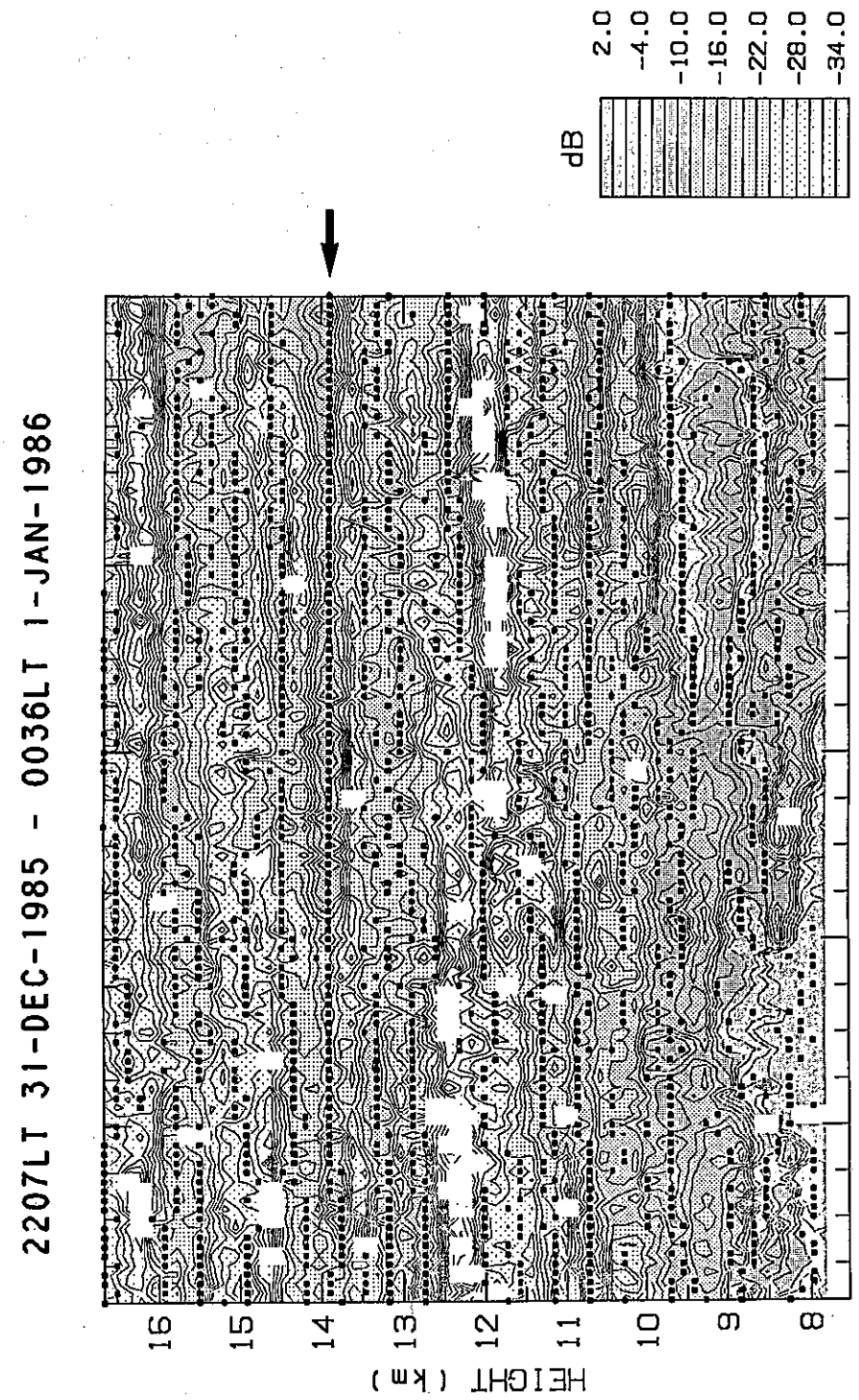

Fig. 14. (*a*) Time height contour of echo intensity. The observation was made from 2207 LT on December 31, 1985, to 0036 LT on January 1, 1986. Dots indicate the heights where the echo intensity profile becomes local maxima. The arrow near 14 km shows that the echo intensity maximum there persists for almost all period of the observation. The beam direction was eastward with an off-zenith angle of 15°. (*b*) Height profile of horizontal wind velocity averaged over the same period as 14*a*. The arrow is put at the same height as in 14*a*.

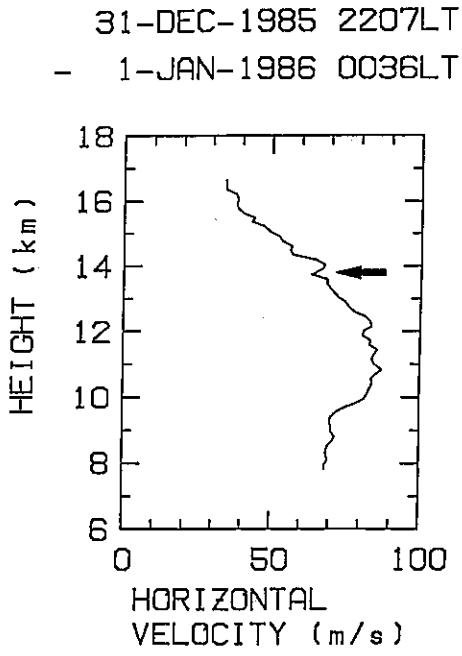

Fig. 14. (continued)

unit range ($\Delta R = 150$ m). Since the eastward jet stream was predominant during this period, the antenna beam was tilted eastward with off-zenith angle of 10° The chain line is the maximum magnitude of positive false wind shear which is theoretically expected in the geometry of Figure 2 for the maximum wind velocity during the present observation. The principal part of the observed distribution seems to be confined below the chain line. As expected, the negative shear is found almost as frequently as the positive shear. The occurrence frequency of negative shear also increases with radial velocity, although the cutoff is not so clearly observed as that of the positive shear.

The critical radial-velocity shears of ± 1.04 $ms^{-1}/\Delta R$, which correspond to ± 40 ms^{-1} km^{-1} of horizontal wind shear, are shown by broken lines in the same figure. Distribution of the observed occurrence frequency is almost confined between these critical values for radial velocity less than 8–10 ms^{-1}. The distribution in the region designated by *B* (shear greater than the maximum theoretical false wind shear and less than the critical radial-velocity shear) is considered to be due mainly to the true wind shears, which exist in the real wind field. On the other hand, it seems impossible to discern the true wind shear for radial velocities larger than 10 ms^{-1}. At least, the principal part in the region *A* (shear greater than the critical radial-velocity shear and less than the maximum theoretical false wind shear) is thought to be false wind shear.

4. OCCURRENCE OF FALSE WIND SHEAR FOR DIFFERENT BEAM WIDTHS

As shown by (1), the radial shear of radial wind velocity (radial-velocity shear) Λ_r is a function of the beam width $\Delta\theta$. The occurrence frequency distribution is obtained by changing the beam width of the MU radar antenna.

The MU radar antenna array consists of 25 subarrays, each of which is composed of 19 yagi antennas [*Fukao et al.*, 1985*a*]. Each subarray can be separately driven, and the antenna beam width can be varied by changing the number of driven subarrays. The shaded areas shown in Figures 7*a*–7*d* indicate the subarrays used, and the corresponding half-power beam widths are approximately 3.7°, 4.2°, 5.2°, and 6.8°, respectively. The antenna beam was directed 10° from the zenith toward the east-northeast (60° in azimuth from the north). Near this azimuth the wind velocity was observed to be maximum. The 1-hour observation sequentially made for each beam width was repeated four times (the total observational period is 16 hours).

The observational result is shown in Figure 8. The maximum radial velocity observed in this period is less than approximately 15 ms^{-1}. The marked cutoff is seen on the positive shear side of the distribution as in Figure 6. It is clearly indicated that the maximum value of the ratio of radial-velocity shear to radial velocity (Λ_r/u_r is shear-velocity ratio) becomes larger for larger beam widths. The radial shear is less than ± 1 $ms^{-1}/\Delta R$ for radial velocity less than a few ms^{-1} in every array configuration.

The maximum shear-velocity ratios Λ_r/u_r estimated by eye from Figure 8 for the four beam widths are plotted against beam width $\Delta\theta$ in Figure 9. The vertical bars show a read error. The result shows that the ratio increases almost linearly with increasing beam width. The observed ratio is less than the theoretical maximum value. This shows that the effective scattering occurs not at the edges of the beam width as considered above but inside the beam width. This point will be more extensively discussed in the accompanying paper [*Fukao et al.*, this issue].

5. FALSE WIND SHEAR FOR DIFFERENT BEAM ZENITH ANGLES

Figure 10 compares the results between two different zenith angles of the antenna beam obtained in a

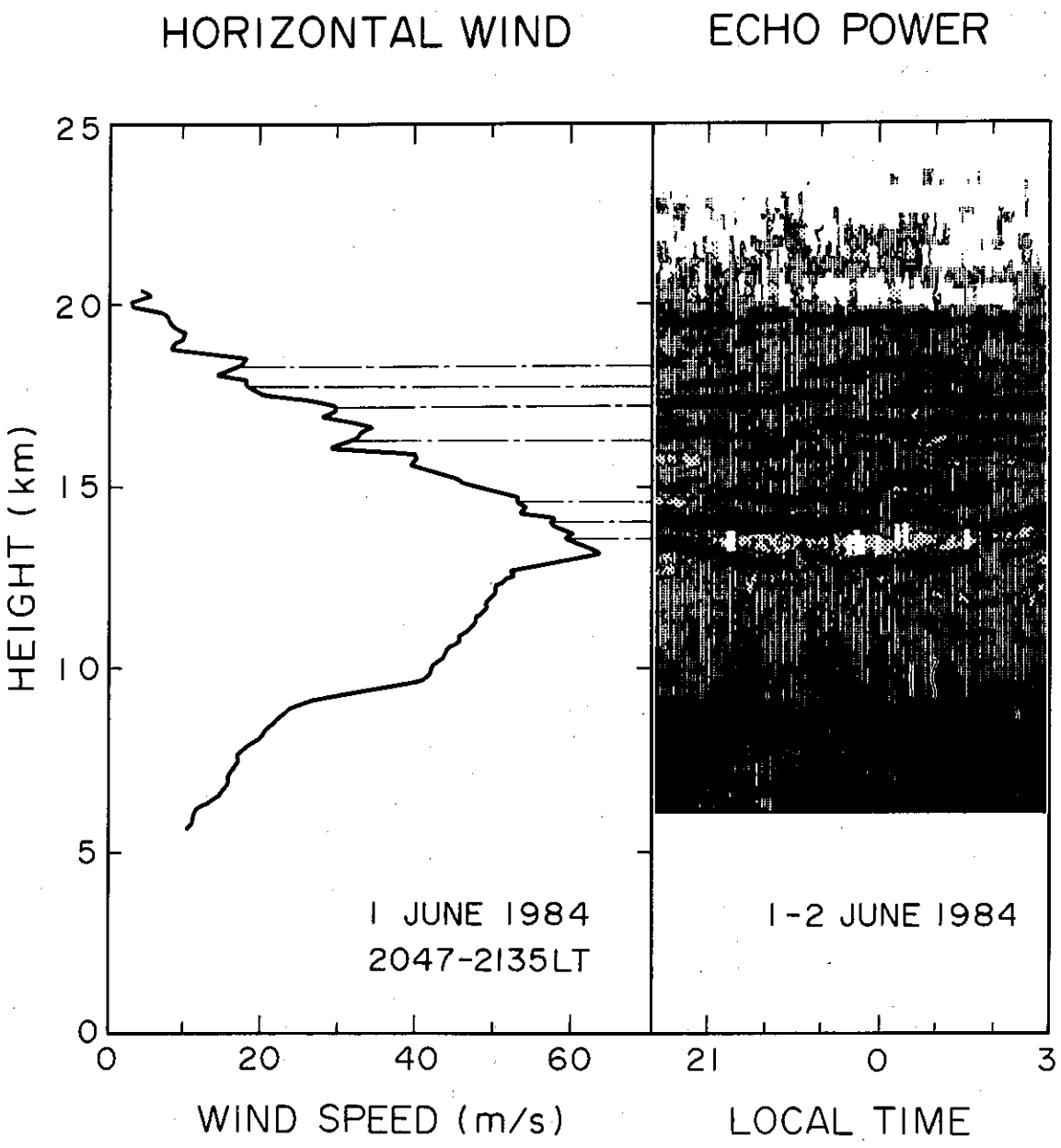

Fig. 15. (left) Horizontal wind averaged over 2047–2135 LT on June 1, 1984. (right) Time height section of echo intensity during a period 2000 LT on June 1 to 0300 LT on June 2, 1984.

2.5-hour period. The antenna beam pointed eastward was changed every alternate pulse to zenith angles of (10*a*) 10° and (10*b*) 15°. The radial wind velocity obtained in the 15° off-zenith direction is multiplied by sin 10°/sin 15°, and this normalized value is used to calculate the radial-velocity shear. The observed shear-velocity ratio is larger in 10*a* than in 10*b*.

The shear-velocity ratio Λ_r/u_r is given as follows;

$$\Lambda_r/u_r = u[\cos\theta \sin(\Delta\theta/2)/\Delta R]/[u \sin\theta]$$
$$= \cot\theta \sin(\Delta\theta/2)/\Delta R \quad (2)$$

This indicates that the shear-velocity ratio is proportional to cot θ for a given $\Delta\theta$. In Figure 10, the observed shear-velocity ratio is 0.14 and 0.09 $ms^{-1}/\Delta R$ for $\theta = 10°$ and 15°, respectively. The ratio of 0.14/0.09 = 1.55 almost coincides with cot 10°/cot 15° = 1.52. The present result suggests that the beam direction should be tilted from the zenith to as large an angle as possible in order to minimize the finite range volume effect. But at large zenith angles it should be allowed that the aspect sensitive scattering deteriorates the signal-to-noise ratio [e.g., *Gage and Balsley*, 1980; *Tsuda et al.*, 1986] and that more than one turbulent layers will be included within a single range volume.

6. FALSE TEMPORAL VARIATION OF WIND

Figure 11 schematically shows another case induced by the finite range volume effect as a turbulent layer moves downward with time within a same range volume (It is beyond the scope of this paper to discuss what changes level of the turbulent layer). This motion gives a false increase of horizontal wind from $u \sin(\theta - \Delta\theta/2)/\sin\theta$ to $u \sin(\theta + \Delta\theta/2)/\sin\theta$ when observed by a radar, although the ambient wind field does not change at all. On the other hand, if the turbulent layer moves upward, the observed wind velocity decreases. The observed temporal variation of wind does not reflect a true wind change but a false one induced by the vertical motion of turbulent layer.

An observational example is shown in Figure 12, where radial wind velocities at three range volumes and echo intensity at five range volumes around 8.86 km are plotted against record number (equivalent to observational time; one record corresponds to approximately 2 min). The velocity change, particularly, during record number 90–100 suggests that a turbulent layer moves from height *A* to *B* of Figure 11. This is considered to produce a false temporal variation of wind velocity, even if the ambient wind does not change. Also, the wind velocity maxima, indicated by arrows, are observed only at the center range volume located at 8.86 km but not at the adjacent two range volumes. Correspondingly, the echo intensity is enhanced at each instance at the lower range volumes. The velocity maxima are probably related to the intense echoes from a turbulent layer which appears at height *B* of Figure 11.

Other similar temporal variations are shown in Figures 13*a* and 13*b*. Note that the velocity scale is approximately two times larger in 13*b* than in 13*a*. The velocity variation observed in 13*a* is quite similar among three adjacent range volumes. The temporal variation that is thought to be a reflection of the finite range volume effect appears only near the record number 40. On the other hand, the wind velocity changes quite differently among three range volumes in 13*b*. The difference between the two cases is presumably referred to the finite range volume effect which is more prominent in larger ambient wind field.

The finite range volume effect sometimes persists for a comparably long time. As an example, a time-height section of echo intensity obtained during a 2.5-hour period is shown in Figure 14*a*. Dots indicate that echo intensity is relatively large compared with adjacent ranges (i.e., local maxima in height profile of echo intensity) at each record number (observational time). At several height ranges, especially near 14 km as indicated by arrow, the dots appear consecutively at the same height for a long duration. The eastward wind profile averaged over the whole observational period is shown in 14*b* of the same figure. Even in this 2.5-hour averaged profile a large wind shear with magnitude greater than 20 ms^{-1} km^{-1} is observed near 14 km where the intense echo persists for a long time. The magnitude often exceeds the critical value of 40 ms^{-1} km^{-1}. The shear is perceived to exist continuously at every record. This shear is presumably false, produced by the finite range volume effect. This result shows that this effect appears not only in individual wind profiles but also in the profiles averaged for a comparably long period. In this sense it is noted that this effect produces more or less a systematic error in the wind velocity measurement by MST/ST radars.

7. DISCUSSIONS AND CONCLUSIONS

In the present paper, a systematic error due to the finite range volume effect for MST/ST radars is discussed, and particular examples are shown from the

MU radar observations. If a turbulent layer is simultaneously located in several adjacent range volumes, this effect leads to a larger wind velocity observed at higher ranges even in a vertically uniform ambient wind field. This false increase of wind velocity appears as a false wind shear, particularly for height ranges where the ambient wind velocity decreases with height. On the other hand, the false wind shear is not so prominent where the ambient wind velocity increases with height.

This feature is most clearly found in the observation by the MU radar as shown in Figure 15. During the period of this observation the jet stream predominated near the tropopause at approximately 13 km. As expected, due to the finite range volume effect several intense wind shears appear above the tropopause where the ambient wind velocity starts to decrease with height. The layered structure of turbulence may be found with velocity-shear magnitudes sometimes larger than the critical value for the onset of turbulence. Although it is not an easy task to show experimentally that turbulent layers are located in configurations such as those illustrated in Figure 2, the good correlation between turbulent layers and wind shears found in Figure 15 suggests that the finite range volume effect is a common feature in the real atmosphere. However, since intense turbulent layers are sometimes observed in strong wind shear regions of the real atmosphere, in practice it will be difficult to precisely discern the true wind shear from the false one in observed data.

The finite range volume effect is primarily determined by the finite beam width of radar antenna as shown in (1). The wider the beam width, the more prominent the false wind shear becomes. The range resolution is not a factor of essential importance for this effect. Further details will be discussed elsewhere [*Fukao et al.*, this issue].

Since turbulence structures are horizontal layers, the finite range volume effect cannot be avoided in any beam directions except the zenith direction. This effect will also cause the same error for velocity azimuth display (VAD) wind measurement by MST/ST radars if turbulence layers cover the VAD circle.

Finally, small vertical scale structure or vertical shear of horizontal wind observed over several height ranges or a few hundred meters should be treated with great care except when the ambient wind field is weak. However, a relatively reliable estimate of wind velocity seems to be provided at heights of local maxima of echo intensity profile compared with heights of minima.

Acknowledgments. The authors are indebted to W. L. Oliver, Jr., of the Radio Atmospheric Science Center, Kyoto University, for his careful reading of the manuscript and valuable comments. The MU radar belongs to and is operated by the Radio Atmospheric Science Center of Kyoto University.

REFERENCES

Atlas, D., R. C. Srevastava, and P. W. Sloss, Wind shear and reflectivity gradient effects on Doppler radar spectra, II, *J. Appl. Meteorol.*, *8*, 384–388, 1969.

Balsley, B. B., and K. S. Gage, The MST radar technique: Potential for middle atmospheric studies, *Pure Appl. Geophys.*, *118*, 452–493, 1980.

Chang, N. J. F., Precision of tropospheric/stratospheric winds measured by the Chatanika radar, *Radio Sci.*, *15*, 371–382, 1980.

Fukao, S., S. Kato, T. Aso, M. Sasada, and T. Makihira, Middle and upper atmosphere radar (MUR) under design in Japan, *Radio Sci.*, *15*, 225–231, 1980.

Fukao, S., T. Sato, N. Yamasaki, R. M. Harper, and S. Kato, Winds measured by a UHF Doppler radar and rawinsondes: Comparisons made on twenty-six days (August–September 1977) at Arecibo, Puerto Rico, *J. Appl. Meteorol.*, *21*, 1357–1363, 1982.

Fukao, S., T. Sato, T. Tsuda, S. Kato, K. Wakasugi, and T. Makihira, The MU radar with an active phased array system, 1, Antenna and power amplifiers, *Radio Sci.*, *20*, 1155–1168, 1985*a*.

Fukao, S., T. Tsuda, T. Sato, S. Kato, K. Wakasugi, and T. Makihira, The MU radar with an active phased array system, 2, In-house equipment, *Radio Sci.*, *20*, 1169–1176, 1985*b*.

Fukao, S., T. Sato, T. Tsuda, S. Kato, M. Inaba, and I. Kimura, VHF-Doppler radar determination of the momentum flux in the upper troposphere and lower stratosphere: Comparison between the three- and four-beam method, *J. Atmos. Oceanic Tech.*, in press, 1988.

Fukao, S., M. Inaba, I. Kimura, P. T. May, T. Sato, T. Tsuda, and S. Kato, A systematic error in MST/ST radar wind measurement induced by a finite range volume effect, 2. Numerical considerations. *Radio Sci.*, this issue.

Gage, K. S., and B. B. Balsley, On the scattering mechanisms contributing to clear air radar echoes from the troposphere, stratosphere, and mesosphere, *Radio Sci.*, *15*, 243–257, 1980.

Gage, K. S., and B. B. Balsley, MST radar studies of wind and turbulence in the middle atmosphere, *J. Atmos. Terr. Phys.*, *46*, 739–753, 1984.

Hocking, W. K., On the extraction of atmospheric turbulence parameters from radar backscatter Doppler spectra, I, Theory, *J. Atmos. Terr. Phys.*, *45*, 89–102, 1983.

Kato, S., T. Ogawa, T. Tsuda, T. Sato, I. Kimura, and S. Fukao, The middle and upper atmosphere radar; First results using a partial system, *Radio Sci.*, *19*, 1475–1484, 1984.

Klostermeyer, J., Computation of acoustic-gravity waves, Kelvin-Helmholtz instabilities, and wave-induced eddy transport in realistic atmospheric models, *J. Geophys. Res.*, *85*, 2829–2839, 1980.

May, P. T., S. Fukao, T. Tsuda, T. Sato, and S. Kato, The effect of thin scattering layers on the determination of wind by Doppler radars, *Radio Sci.*, this issue.

Röttger, J., The MST radar technique, in *Handbook for MAP*, vol. 13, edited by R. A. Vincent, pp. 187–232, University of Illinois, Urbana, Ill., 1984.

Röttger, J., and G. Schmidt, High-resolution VHF radar sounding

tron., GE-17, 182–189, 1979.

Sato, T., and S. Fukao, Altitude smearing due to instrumental resolution in MST radar measurements, *Geophys. Res. Lett.*, *9*, 72–75, 1982.

Tsuda, T., T. Sato, K. Hirose, S. Fukao, and S. Kato, MU radar observations of the aspect sensitivity of the backscattered VHF echo power in the troposphere and lower stratosphere, *Radio Sci.*, *21*, 971–980, 1986.

Warnock, J. M., T. E. VanZandt, J. L. Green, and R. H. Winkler, Comparison between wind profiles measured by Doppler radar and by rawinsonde balloons, *Geophys. Res. Lett.*, *5*, 109–112, 1978.

Waterman, A. T., T-z. Hu, P. Czechowsky, and J. Röttger, Varia-

case study, *Radio Sci.*, [illegible]

Watkins, B. J., and P. E. Johnston, Antenna-induced range smearing in ST and MST radars, *Radio Sci.*, *20*, 1130–1140, 1985.

Woodman, R. F., High-altitude resolution stratospheric measurements with the Arecibo 430-MHz radar, *Radio Sci.*, *15*, 417–422, 1980.

S. Fukao, S. Kato, P. T. May, T. Sato, and T. Tsuda, Radio Atmospheric Science Center, Kyoto University, Uji, Kyoto 611, Japan.

M. Inaba and I. Kimura, Department of Electrical Engineering, Kyoto University, Yoshida, Kyoto 606, Japan.